Energy Reports 8 (2022) 7374–7385

Contents lists available at ScienceDirect

Energy Reports

journal homepage: www.elsevier.com/locate/egyr

Research paper

Two-stage optimization of a virtual power plant incorporating with demand response and energy complementation

Jinye Cao [a], Yingying Zheng [a], Xueru Han [a], Dechang Yang [a,*], Jianshu Yu [a], Nikita Tomin [b], Payman Dehghanian [c]

[a] College of Information and Electrical Engineering, China Agricultural University, Beijing, 100083, China
[b] The Siberian Branch of the Russian Academy of Sciences-Melentiev Energy Systems Institute, Russia
[c] Department of Electrical and Computer Engineering, George Washington University (GWU), USA

ARTICLE INFO

Article history:
Received 26 February 2022
Received in revised form 14 May 2022
Accepted 25 May 2022
Available online xxxx

Keywords:
Virtual power plant
Demand response
Energy complementation
Scheduling strategy
Uncertainty

ABSTRACT

The virtual power plant (VPP) breaks the geographical restrictions of environment and resource types by virtue of aggregating the distributed energy resources and dispatchable loads. In view of the impact of large-scale energy consumption by users on the operational safety of VPP, based on the existing demand response (DR) researches, this paper adds a penalty mechanism for the reasonable management of loads. For the difference of resources in multiple VPPs, the current researches ignore the energy interaction between different VPPs, and the external operator is introduced innovatively in this paper to coordinate the real-time complementation of regional energy. Considering the uncertainty from renewable energy and load, a two-stage scheduling strategy for VPP with multi-time scale optimization is proposed, including a long-time scale day-ahead scheduling and a short-time scale real-time scheduling. On the basis of DR and unit constraints, the resource scheduling plan is formulated in the day-ahead stage. In the real-time stage, the energy complementation between VPPs is considered under the framework of rolling optimization for the correction of the previous plan. The scheduling of both stages is aimed at the economic operation of the VPP. Simulation results show that the DR flexibly optimizes the load distribution while bringing economic benefits, and the total profit can be increased by up to 6.65%. Moreover, the results show that the energy interaction under the external operator coordination significantly reduces the total correction cost by up to 8.23%, and the correction cost is decreased with the extension of the rolling optimization scheduling period.

1. Introduction

The world is transforming its energy system from one dominated by fossil fuel combustion to one with net-zero emissions of carbon dioxide (CO_2) and primarily composed of a large amount of distributed energy resources (DER). The Chinese government has committed to peak CO_2 emissions by 2030, reducing CO_2 emissions per unit of GDP by 60%–65% from 2005 levels (Sheng et al., 2021). Compared with the centralized power generation, DER has the advantages of economy, flexibility, environmental protection, reliability and other aspects. Therefore, the research on the effective utilization of DER is of great practical value.

However, the strong intermittent behaviors in the cumulative power generation of DER bring negative impacts on grid integration (Yang et al., 2019). In addition, the small capacity and geographically dispersed locations make DER difficult to be regulated accurately by the power grid (Wang and Wu, 2021). To address those challenges, virtual power plant (VPP), serves as an aggregator that facilitates the interaction between the DERs and the distribution level energy consumers is developed. VPP has the functions of power generation, distribution, sale, and purchase, it can participate in the electricity market as an independent power retailer (Zhang et al., 2019). The successful implementation of VPP relies on reasonable scheduling of internal resources, such as micro-gas turbines, fuel cells, and dispatchable loads (Zhou et al., 2016). Hence, the scheduling strategy of VPP becomes a research hotspot (Ju et al., 2019).

Hadayeghparast et al. (2019) proposed a multi-objective operational scheduling of DER in VPP based on the expected day-ahead benefits and emission. Akkaş and Çam (2020) explored the day-ahead adjustment of the entire generation system of VPP. In Shayegan-Rad et al. (2017), a day-ahead scheduling framework for VPP in a joint energy and regulation reserve markets was presented. Zamani et al. (2016a) explored a probabilistic model for optimal day-ahead scheduling of electrical and thermal energy

* Correspondence to: College of Information and Electrical Engineering, China Agricultural University, No.17, Tsinghua East Road, Haidian District, Beijing, China.
E-mail address: yangdechang@cau.edu.cn (D. Yang).

https://doi.org/10.1016/j.egyr.2022.05.255

resources in a VPP. Yuan et al. (2014) illustrate a real-time control strategy in dispatching active power among units to balance the power deviation. In Zhu et al. (2019), the real-time economic dispatch of VPPs was studied on the basis of various interests of VPPs and a system operator. Most of the VPP optimal dispatch researches focus on either the day-ahead scheduling or real-time scheduling, whereas the combination of different scheduling strategies for all scheduling stages is limited.

The massive consumption of DERs in VPPs urgently requires the research on demand response (DR) of users for the effective demand side scheduling. DR is a program that compensates the power consumers for reducing or transferring the power load during peak hours of electricity usage, and the program is preset in the form of contracts (Yang et al., 2021). In addition, user satisfaction with electricity consumption is a key indicator to measure the effect of DR (Mishra et al., 2019). Chen et al. (2021) constructed the electricity consumption satisfaction function and set different compensatory prices to dispatch residential loads. Aalami et al. (2010) developed an extended responsive load model based on DR contracts to improve load profile characteristics and user satisfaction. In Royapoor et al. (2020), a commercial building was selected as the VPP and various dispatchable loads including air conditioners, lighting, and pumps were used to illustrate building's DR capability. In Vahedipour-Dahraie et al. (2021), the curtailment and shift options for dispatchable loads were used by customers under DR contracts to minimize the consumption costs. These studies have confirmed that DR plays an important role in the interactions between energy users and VPP, that is, flexibly optimizes the load distribution on the premise of ensuring user satisfaction. However, the current studies on DR contracts mainly focus on the compensation mechanism for users, and rarely consider the penalty mechanism for the over-responsiveness of users, which would exacerbate load fluctuations in some periods.

The scheduling strategy of VPP is based on forecast data, therefore, the uncertainties from wind power, solar power, and load cannot be ignored (Zamani et al., 2016b). The robust optimization (RO), distributionally robust optimization (DRO), scenario-based method, and model predictive control (MPC) method are common solutions to deal with uncertainties. RO uses the boundary information of uncertainties to form an uncertainty set, and selects the worst scenario in the uncertainty set for optimal decision-making (Du et al., 2019). Compared to RO with uncertainty sets, the probabilistic modeling of uncertainty is required for DRO (Zhou et al., 2021). Due to the difficulty of incorporating analytical probabilistic models into the optimization model, limited discrete scenarios are used to replace the probabilistic model in the DRO solution process (Du et al., 2021). Whereas the scenario-based method can reduce the computational complexity caused by large numbers of discrete scenarios, and effectively improve the computational efficiency of optimization problems (Vagropoulos et al., 2016). Compared with uncertainty sets, discrete scenarios obtained by the scenario-based method can bring more reliable and stable decision-making solutions in power system uncertainty optimization (Seljom et al., 2021). On short time scales, MPC has unique advantages in dealing with uncertainties due to its rolling optimization mechanism based on the updated data (Grimm et al., 2021).

In recent years, researchers have carried out in-depth researches on the scenario-based method and MPC. However, in the existing researches, the method of modeling uncertainty in multi-time scale is relatively single, which is manifested as adopting the same method in different time scales. Wang et al. (2021) explored the application of scenario generation and reduction methods in wind speed simulation. Naughton et al. (2020) presented a scenario-based approach to operating a multi-energy VPP under uncertainty. In Ju et al. (2016), a scenario-based frame was proposed for analyzing the output of photovoltaic generators and wind power plants. In Nguyen et al. (2018), a scenario-based optimization approach was used to solve a three-stage stochastic program. Castillo et al. (2019) studied the application of MPC in hourly scheduling of VPP operators by rolling optimization. Xiao et al. (2020) conducted the rolling optimization of spot price through MPC. Considering compressed air energy storage wind turbine, Rahimi et al. (2022) introduced the MPC applied in the day-ahead and real-time scheduling. In Yi et al. (2020), the day-ahead bidding and real-time operation were both achieved by the MPC. Therefore, in the multi-time scale optimization, there is a lot of research space to study the combination of uncertainty processing methods based on different time scales.

Moreover, due to the interference from uncertainty, for two adjacent scheduling stages, the previous dispatch plan would be corrected by the latter stage. To balance the deviation, Mohy Ud Din et al. (2019) proposed an idea of the information and power exchange between VPPs in the real-time market. In Jha et al. (2021), a collaborative scheduling model of VPPs was established, but the energy interactions between VPPs is not considered in this model. In Lyu and Wang (2019), the peer-to-peer mechanism of power trading between VPPs was designed, whereas this direct transaction mechanism has the risk of disorder due to the lack of operator management. Overall, there are few studies on the external operator coordinating the interactions between VPPs, and the current research on the VPP operator is limited to the role of internal aggregation resources dispatch. For example, in Asl et al. (2021), an energy management model was established to coordinate the distribution of benefits between VPP operator and distributed renewable resources, and in Vahedipour-Dahraie et al. (2020), the effects of the VPP operator's risk-averse behavior on the VPP internal energy and its security performance were investigated. Therefore, in view of the successful application of the operator for energy coordination and complementation in the intelligent building cluster (IBC) (Dou et al., 2021), intelligent residential communities (Huang, 2014), and integrated energy system (IES) (Yu et al., 2021; Yan et al., 2019), the VPP cluster operator (VPPCO) would be introduced to effectively coordinate and manage the energy and information interaction among multiple VPPs.

Based on the above analysis, the optimization scheduling of VPP still has a lot of research space. It is embodied in: the joint dispatch of VPP in multi-scheduling stages, the combined use of scenario-based approach and MPC method to address the uncertainty, the coordination role of VPPCO for interactions between VPPs, and the optimization role of DR for interactions between VPP and energy users. In response to these problems, this paper proposes a two-stage scheduling strategy for VPP with multi-time scale optimization, which consists of a long-time scale day-ahead scheduling and a short-time scale real-time scheduling. The main contributions of this paper are summarized as follows.

(1) Considering the uncertainty of wind power, photovoltaics, and load, the scenario-based approach is used in the day-ahead scheduling to form a preliminary dispatch plan. Based on the MPC method, the real-time scheduling corrects the day-ahead scheme through rolling optimization on a reduced time scale.

(2) An improved DR program is developed in this paper, which takes fully account of both the compensation and penalty mechanism in the form of bilateral contract between VPP and energy users for a reasonable response.

(3) The concept of VPPCO is proposed in this paper, which provides a platform in the real-time stage for the energy and information interactions between VPPs. The VPPCO will be beneficial for the energy coordination and complementation while reducing correction costs for real-time scheduling.

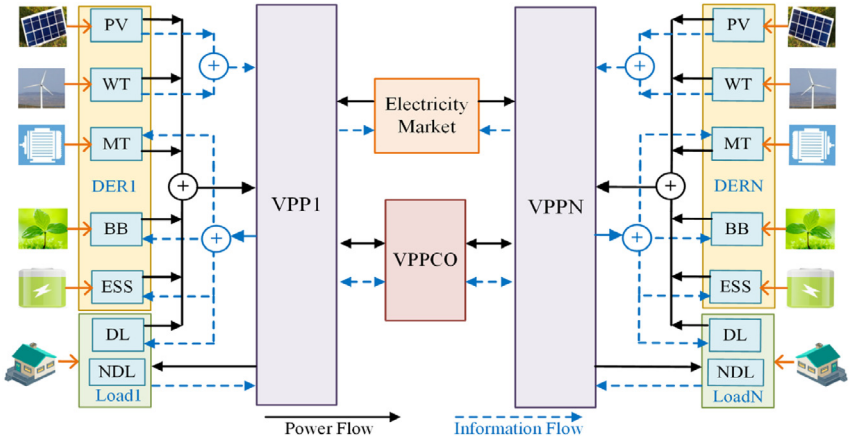

Fig. 1. The VPP operational structure.

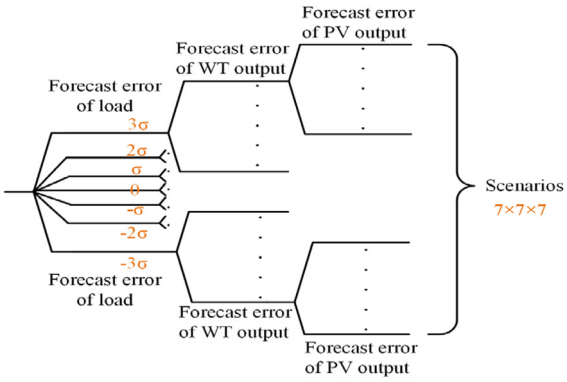

Fig. 2. The structure of scenario set generation tree.

The remainder of the paper is organized as follows: Section 2 introduces the structure of VPP and its optimization method, including the operational structure of VPP, and the frameworks of scenario-based approach and multi-time scale optimization. Section 3 establishes mathematic models of VPP including objective functions and constraints. Case study and result analysis are presented in Section 4. Section 5 draws the conclusion.

2. The structure of VPP and its optimization methods

2.1. Operational structure of VPP

In terms of the scheduling objects of VPP, the power load can be divided into dispatchable load (DL) and non-dispatchable load (NDL), and the internal aggregation resources can be characterized as controllable ones and non-controllable ones. In this paper, micro-gas turbines (MT), biomass boilers (BB), dispatchable load (DL), and energy storage system (ESS) are the controllable units, whereas photovoltaics (PV) and the wind turbines (WT) are the non-controllable units. The operation framework of VPP is shown in Fig. 1. As shown in Fig. 1, based on the uploaded forecast information from PV, WT, and load, the VPP dispatches its controllable units and purchases power in the electricity market to meet the demand of energy users. Acting as an intermediary for the real-time transaction, the VPPCO collects the power information of each VPP, and coordinates energy exchanges between VPPs according to the principle of energy complementarity. For a VPP with excess power in the real-time stage, the surplus electricity is sold to other VPPs with insufficient power through VPPCO, and each VPP participating in energy complementation is required to pay an agency fee to the VPPCO for its service. In addition, due to the constraint from the power line transmission capacity, the power exchange is limited.

2.2. Framework of scenario-based approach

In this paper, the load, and the power output of WT and PV are treated as uncertainties and stochastic parameters, and the combination of the three uncertainties constitutes the scenario set. To transform the stochastic optimization problem into a deterministic one, a scenario-based approach involving scenario set generation, selection, and elimination is adopted in the day-ahead scheduling.

2.2.1. Scenario set generation method

The forecasted value of uncertainty is obtained from historical data and the forecast error is determined by the corresponding probability density function (PDF). According to the three-sigma rule in normal distribution, the range of three times positive and negative standard deviations can contain 99.7% of the likely scenarios. In this paper, the forecast error follows normal distribution, the PDF of which with 0 as the mean is divided into seven levels, namely, 0, $\pm 1\sigma$, $\pm 2\sigma$, $\pm 3\sigma$, and σ denotes the standard deviation of uncertainty. The roulette wheel mechanism (RWM) and Lattice Monte Carlo Simulations (LMCS) are applied to achieve the hourly scenario generation for each stochastic parameter (Niknam et al., 2012), and the forecasted value is updated after adding the corresponding forecast error of each scenario. Fig. 2 illustrates the generation process of scenario set in the form of a tree, the number of which generated in an hour is $7^3 = 343$.

2.2.2. Scenario set elimination method

To realize the elimination of scenario sets, the forward selection (FS) technology is applied. Initially, only one scenario set is retained, and the number of sets increases with the FS operations. For each selection, the probability distance between the retained and the selected scenario set would be the shortest, and the probability of each scenario set is assigned according to the distance between scenario sets (Gomes et al., 2021). The SCENRED provided by GAMS is used for the scenario elimination, and typical ones have been selected from the 343 scenario sets in each hour. After the scenario elimination, the probability of each scenario set is multiplied by the corresponding forecasted values and summed to obtain the final values of uncertainties per hour.

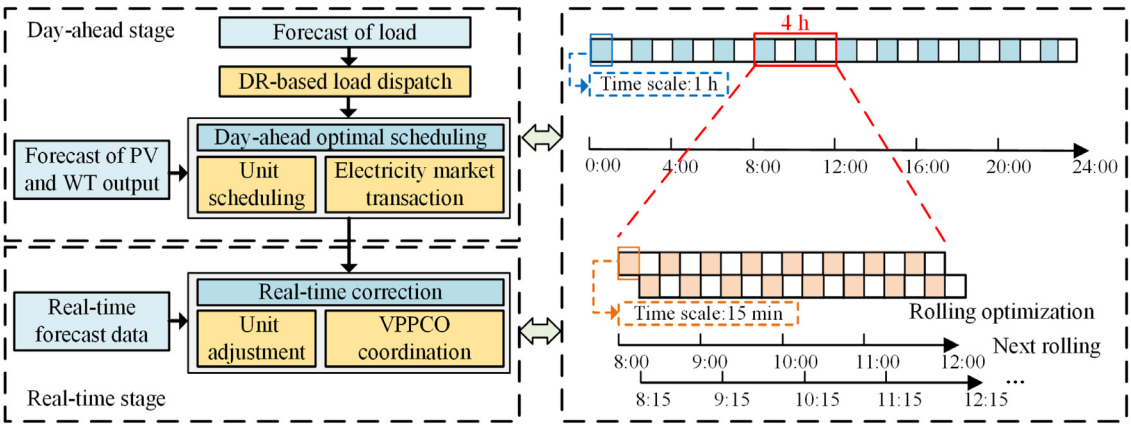

Fig. 3. The flow chart of two-stage scheduling with multi-time scale optimization.

2.3. Framework of multi-time scale optimization

The multi-time scale optimization including the long-time scale optimization in day-ahead stage and the short-time scale rolling optimization in real-time stage are shown in Fig. 3. For the day-ahead stage with 24 h of scheduling period and 1 h of time scale, it can be subdivided into two steps. The first step is to optimize the power load distribution by means of the DR-based load dispatch, and the second step is to formulate the scheduling plan of each controllable unit and the transaction plan in the electricity market based on the short-term forecast data. Compared to the one-time optimization in day-ahead stage, the rolling optimization achieved by the MPC method schedules more precisely by reducing time granularity (Zheng et al., 2018). In this paper, the time scale of real-time rolling optimization is set as 15 min, the scheduling period is 4 h, and the total number of optimization periods in a day is 96. Specifically speaking, for a scheduling period, based on the uploaded ultra-short-term forecast data for 16 time periods, the VPP corrects the previous scheduling schemes by adjusting the output of the aggregated units and trading power with other VPPs through VPPCO, whereas only the decisions that made in the first time period are going to be executed. As shown in Fig. 3, the whole real-time scheduling process is optimized on a rolling basis.

3. Two-stage optimization model for VPP

3.1. DR model in the day-ahead stage

3.1.1. Objective function

According to the dispatch form of DR, the DL can be divided into shiftable load (SL) and interruptible load (IL). In this paper, the compensation and penalty mechanism are developed with the electricity price that stipulated in a bilateral contract, consisting of benchmark price, compensation price and penalty price, which takes place of the traditional time-of-use price. To be more specific, users purchase power with the benchmark price, and driven by the benchmark price signals, they can spontaneously shift loads to other time periods. Under the incentive of the compensation price, they would interrupt part of their loads as scheduled. Moreover, to ensure the reasonable response of loads and the operational safety of VPP, the range of hourly power consumption is set by the contract based on the forecasted value, and the penalty price would be added to users in case of the excessive load shift and interruption. In this paper, the satisfaction of users, which is applied to reflect the effect of DR, depends on the power purchase cost change. The objective function is formulated as follows:

$$\max I^i = 1 - \frac{\sum_{t=1}^{T}\sum_{s=1}^{S} H_{t,s}^i \left(P_{rp,t,s}^i W_{bp,t} - P_{cu,t,s}^i W_{dr,t} + P_{eva,t,s}^i W_{pen,t}\right)}{\sum_{t=1}^{T}\sum_{s=1}^{S} H_{t,s}^i P_{l,t,s}^i W_{tou,t}^i} \tag{1}$$

$$P_{eva,t,s}^i = \begin{cases} P_{cp,t,\min}^i - P_{rp,t,s}^i & P_{rp,t,s}^i < P_{cp,t,\min}^i \\ P_{rp,t,s}^i - P_{cp,t,\max}^i & P_{rp,t,s}^i > P_{cp,t,\max}^i \\ 0 & else \end{cases} \tag{2}$$

where i is the VPP number; t is the time step; T is the length of the planning horizon; s is the scenario set number; S is the volume of scenario sets; $H_{t,s}^i$ is the probability of scenario set s at time t; I^i reflects the degree of user satisfaction in VPPi; $P_{l,t,s}^i$ is the forecast load of VPPi at time t in scenario set s; $W_{tou,t}^i$ is the time-of-use price of VPPi at time t; $P_{rp,t,s}^i$ is the actual load of VPPi after DR at time t in scenario set s; $W_{bp,t}$ is the benchmark price at time t; $P_{cu,t,s}^i$ denotes the IL of VPPi at time t in scenario set s; $W_{dr,t}$ is the compensation price at time t; $P_{eva,t,s}^i$ denotes the electricity usage deviation to be punished by VPPi at time t in scenario set s; $P_{cp,t,\min}^i$ and $P_{cp,t,\max}^i$ are the minimum and maximum hourly allowed power consumption restricted by VPPi at time t; $W_{pen,t}$ is the penalty price at time t.

3.1.2. Constraints

(1) Balance constraint of dispatchable load

As mentioned above, the DL can be transferred or interrupted correspondingly in compliance with DR, and the balance constraint is as follow:

$$P_{rp,t,s}^i = P_{l,t,s}^i - P_{cu,t,s}^i - \left(P_{tran,t,s}^i - P_{trap,t,s}^i\right) \tag{3}$$

where $P_{tran,t,s}^i$ denotes the SL of VPPi in scenario set s transferred from time t to other time periods, and $P_{trap,t,s}^i$ denotes the SL transferred from other time periods to time t.

(2) Balance constraint of shiftable load

The total transferred-volume of SL, including load transferred-in and transferred-out, is zero within a planning horizon. The equation of SL transferred in a planning horizon is:

$$\sum_{t=1}^{T} P_{tran,t,s}^i - \sum_{t=1}^{T} P_{trap,t,s}^i = 0 \tag{4}$$

(3) Upper and lower limits of interruptible load and shiftable load

Constraints (5)–(7) restrict the dispatch range of IL and SL.

$$0 \le P_{cu,t,s}^i \le U_{a,t}^i \partial_{cu}^i P_{l,t,s}^i \tag{5}$$

$$0 \le P^i_{trap,t,s} \le U^i_{b,t}\partial^i_{tra}P^i_{l,t,s} \tag{6}$$

$$0 \le P^i_{tran,t,s} \le U^i_{c,t}\partial^i_{tra}P^i_{l,t,s} \tag{7}$$

where $U^i_{a,t}$ is a binary variable determines the dispatch of IL at time t; 1 means the load interrupted, 0 means no load being interrupted; $U^i_{b,t}$ and $U^i_{c,t}$ are binary variables that represent the load transferred in or out at time t, respectively; 1 means the load is shifted, and 0 means no load is shifted; ∂^i_{cu} denotes the maximum proportion of IL in VPPi at time t, and ∂^i_{tra} denotes the maximum proportion of SL in VPPi at time t.

(4) Dispatch constraints of interruptible load and shiftable load

To reduce the negative impact from sacrificing the user satisfaction in changing the power consumption behavior, the maximum number of dispatch and consecutive dispatch of IL within one planning horizon is limited. Due to the process of load shift is spontaneous, the maximum number of dispatch of SL within one planning horizon would also be restricted for orderly transfer. In addition, the SL cannot carry out the load transferred-out and transferred-in simultaneously at time t. Constraints of IL and SL dispatch are shown in (8)–(9) and (10)–(11), respectively:

$$\sum_{t=1}^{T} U^i_{a,t} \le L_{cu,\max} \tag{8}$$

$$\sum_{t=t_0}^{t+T_{cu,\max}} U^i_{a,t} \le T_{cu,\max} \qquad m \in [1, T-T_{cu,\max}] \tag{9}$$

$$\sum_{t=1}^{T}(U^i_{b,t} + U^i_{c,t}) \le L_{tra,\max} \tag{10}$$

$$U^i_{b,t} + U^i_{c,t} \le 1 \tag{11}$$

where $L_{cu,\max}$ and $L_{tra,\max}$ denote the maximum number of dispatches for IL and SL; $T_{cu,\max}$ is the maximum number of consecutive dispatches for IL.

3.2. VPP optimal scheduling model in the day-ahead stage

3.2.1. Objective function

Fig. 4 illustrates the money flow apropos VPP, electricity market, and energy users participating in DR. As shown in Fig. 4, the revenue of VPP comes from the power sale income (A) and the penalty of users for DR contract breach (B), the cost originates in the compensation for load interruption of users (C), the power purchase expenditure in the electricity market (D), and the internal operating expenses which includes the environmental cost (E)-(F), MT operating cost (G)-(H), BB operating cost (I)-(J), and ESS rental cost (K). The objective function of VPP optimal scheduling in the day-ahead optimization is the maximum profit, which can be calculated as follows:

$$\max R^i = \sum_{t=1}^{T}\sum_{s=1}^{S} H^i_{t,s}\left(P^i_{rp,t,s}W_{bp,t} + P^i_{eva,t,s}W_{pen,t} - P^i_{cu,t,s}W_{dr,t} - P^i_{buy,t}W_{buy,t}\right) - \sum_{t=1}^{T} C^i_{vpp,t} \tag{12}$$

$$C^i_{vpp,t} = C^i_{en,t} + C^i_{mt,t} + C^i_{bio,t} + C^i_{ess,t} \tag{13}$$

where R^i represents the profit gained by VPPi; $P^i_{buy,t}$ represents the power purchased in the electricity market at time t; $W_{buy,t}$ represents the power purchase price at time t; $C^i_{vpp,t}$ represents the operation cost of VPPi at time t; $C^i_{en,t}$, $C^i_{mt,t}$, $C^i_{bio,t}$, and $C^i_{ess,t}$ denote the cost of pollution emission, MT operating, BB operating and ESS rent at time t, respectively.

Due to both MT and BB emit carbon dioxide, sulfide, and nitride during operation, the pollution emission penalty of VPP is calculated as follow:

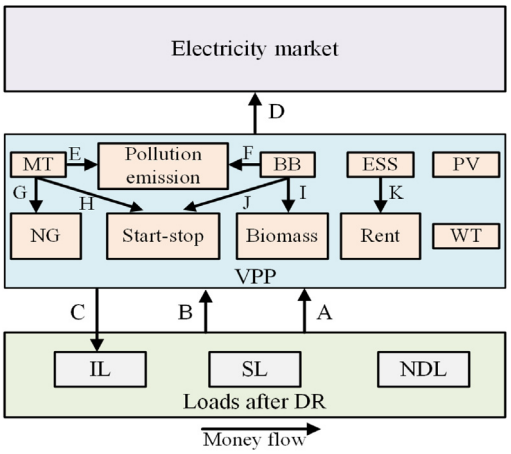

Fig. 4. The structure of money flow.

$$C^i_{en,t} = P^i_{mt,t}\left(\theta_{mt,SO_2}C_{SO_2} + \theta_{mt,NOX}C_{NOX} + \theta_{mt,CO_2}C_{CO_2}\right) + P^i_{bio,t}\left(\theta_{bio,SO_2}C_{SO_2} + \theta_{bio,NOX}C_{NOX} + \theta_{bio,CO_2}C_{CO_2}\right) \tag{14}$$

where $P^i_{mt,t}$ and $P^i_{bio,t}$ are the output of MT and BB in VPPi; θ_{mt,SO_2}, $\theta_{mt,NOX}$, θ_{mt,CO_2}, and θ_{bio,SO_2}, $\theta_{bio,NOX}$, θ_{bio,CO_2} denote the emission factors of SO_2, NOX, and CO_2 of MT and BB at time t, respectively; C_{SO_2}, C_{NOX}, and C_{CO_2} denote the externality cost of SO_2, NOX, and CO_2 pollution.

To improve the flexibility and economy of optimization, the start–stop plans of MT and BB considering the intermittent power generation are scheduled in this paper, and the change of operating status would incur additional costs. As illustrated in Fig. 4, the operation costs of MT and BB composes of start–stop costs, (H) and (J), as well as raw material costs for natural gas (NG) and biomass consumption, (G) and (I), which can be calculated in (15)–(16).

$$C^i_{mt,t} = \frac{P^i_{mt,t}}{n_1 k_1}W_{gas} + U^i_{smt,t}W_{smt} \tag{15}$$

$$C^i_{bio,t} = \frac{P^i_{bio,t}}{n_2 k_2}W_{bio} + U^i_{sbio,t}W_{sbio} \tag{16}$$

where n_1 and n_2 represent the generating efficiency of MT and BB in VPPi; k_1 and k_2 represent the low heating value (LHV) of NG and biomass; $U^i_{smt,t}$ and $U^i_{sbio,t}$ denote the binary variables determining the start–stop state of MT and BB at time t, 1 means that there exists the change of operation state at time t, 0 means no change in operation state at time t; W_{smt} and W_{sbio} denote the start–stop costs of MT and BB.

In addition, both the charging and discharging status of ESS are controlled to stabilize the uncertainty and volatility of renewable energy output. The rental cost of ESS is as follow:

$$C^i_{ess,t} = (P^i_{ess,dis,t} + P^i_{ess,ch,t})W_{rent} \tag{17}$$

where $P^i_{ess,dis,t}$ and $P^i_{ess,dis,t}$ denote the power discharged or charged in VPPi at time t; W_{rent} is the rental cost per unit of capacity.

3.2.2. Constraints

(1) Electricity balance constraint of VPP

Eq. (18) shows the electricity balance during the operation of VPP, which considers the power transaction, generation, and storage.

$$P^i_{rp,t,s} = P^i_{buy,t} + P^i_{wt,t,s} + P^i_{pv,t,s} + P^i_{bio,t} + P^i_{mt,t} + P^i_{ess,dis,t} - P^i_{ess,ch,t} \tag{18}$$

where $P^i_{wt,t,s}$ is the day-ahead forecast output of WT in VPPi at time t in scenario set s; $P^i_{pv,t,s}$ is the day-ahead forecast output of PV in VPPi at time t in scenario set s;

(2) Upper and lower limits of power purchase

In the day-ahead stage, the VPP enters into a power purchase contract with the electricity market, which is subject to the following constraint:

$$P^i_{buy,\min} \le P^i_{buy,t} \le P^i_{buy,\max} \tag{19}$$

where $P^i_{buy,\max}$ and $P^i_{buy,\min}$ are the upper and lower limits of the power purchased by VPPi in the electricity market.

(3) Operational constraints of the micro-gas turbine

Constraint (20) restricts the hourly output of MT, constraint (21) restricts the ramping and descending rate of MT and constraint (22) indicates the relationship between the start–stop action and the operation state of MT.

$$U^i_{mt,t}P^i_{mt,\min} \le P^i_{mt,t} \le U^i_{mt,t}P^i_{mt,\max} \tag{20}$$

$$-k^i_{rd,\max} \le P^i_{mt,t+1} - P^i_{mt,t} \le k^i_{ru,\max} \tag{21}$$

$$U^i_{mt,t} - U^i_{mt,t-1} \le U^i_{smt,t} \tag{22}$$

where $U^i_{mt,t}$ is the binary variable determining the operation state of MT in VPPi at time t, 1 means the start state, and 0 means the stop state; $P^i_{mt,\min}$ and $P^i_{mt,\max}$ denote the minimum and maximum power output of MT in VPPi; $k^i_{ru,\max}$ is the maximum ramping rate of MT in VPPi; $k^i_{rd,\max}$ is the maximum descending rate of MT in VPPi.

(4) Operational constraints of the biomass boiler

Constraint (23) restricts the hourly output of BB. Constraint (24) restricts its start–stop action and operation state.

$$U^i_{bio,t}P^i_{bio,\min} \le P^i_{bio,t} \le U^i_{bio,t}P^i_{bio,\max} \tag{23}$$

$$U^i_{bio,t} - U^i_{bio,t-1} \le U^i_{sbio,t} \tag{24}$$

where $U^i_{bio,t}$ is the binary variable determining the operation state of BB in VPPi at time t, 1 means the state of start, 0 means the state of stop; $P^i_{bio,\min}$ and $P^i_{bio,\max}$ denote the minimum and maximum power output of BB in VPPi.

(5) Energy balance constraints of the energy storage system

The state of charge (SOC) of ESS at time t is a function of SOC at the previous time $t-1$, and the final SOC would be equal to the initial SOC. The constraints are as follows:

$$P^i_{ess,t} = P^i_{ess,t-1} - \frac{P^i_{ess,dis,t-1}}{\eta_{dis}} + P^i_{ess,ch,t-1}\eta_{ch} \tag{25}$$

$$P^i_{ess,t=0} = P^i_{ess,t=24} \tag{26}$$

$$E^i_r SOC_{\min} \le P^i_{ess,t} \le E^i_r SOC_{\max} \tag{27}$$

where $P^i_{ess,t}$ denotes the energy stored of ESS in VPPi at time t; η_{dis} is the discharging efficiency of ESS; η_{ch} is the charging efficiency of ESS; E^i_r is the rated capacity of ESS in VPPi; $SOC_{\min}$ and $SOC_{\max}$ are the minimum and maximum storage state of ESS, respectively.

(6) Input and output constraints of the energy storage system

It should be noted that ESS cannot be charged and discharged at the same time, the hourly output and input of ESS are limited by constraints (28)–(30).

$$0 \le P^i_{ess,ch,t} \le U^i_{ch,t}E^i_r SOC_{\max} \tag{28}$$

$$0 \le P^i_{ess,dis,t} \le U^i_{dis,t}E^i_r SOC_{\max} \tag{29}$$

$$U^i_{dis,t} + U^i_{ch,t} \le 1 \tag{30}$$

where $U^i_{ch,t}$ and $U^i_{dis,t}$ are binary variables determining the state of charge and discharge of ESS in VPPi at time t, 1 means the ESS is charged or discharged, and 0 means no charge or discharge.

3.3. Correction model in the real-time stage

3.3.1. Objective function

Due to the deviations between the day-ahead and real-time forecasts of WT, PV output, and power load, there will be a difference between the scheduling plan and the actual operation, it is necessary to correct the day-ahead scheduling plan. For a VPP, the forecast deviations are counterbalanced by the adjustment of MT and BB output, as well as the energy interaction with other VPPs. Given the impact of frequent charge and discharge operations on the battery life caused by the rolling optimization, the correction to ESS is not considered in the real-time scheduling. In addition, since the load dispatch and electricity market transaction plans have been previously determined in the form of contracts, they are no longer real-time corrected. As mentioned above, the power trading between VPPs is coordinated uniformly by the VPPCO to realize the complementarity of the surplus or insufficient power of each VPP, the objective function is the minimum correction cost, which is formulated as follow:

$$\begin{aligned}\min C^i_{rev} = \sum_{t=t_0}^{t+\Delta T}[\beta_1 \sum_{k=1,k\neq i}^{N}(P^i_{vppin,t,k} + P^i_{vppout,t,k}) \\ + \beta_2 \sum_{k=1,k\neq i}^{N} P^i_{vppin,t,k} - \beta_3 \sum_{k=1,k\neq i}^{N} P^i_{vppout,t,k} + C^i_{mtrev,t} + C^i_{biorev,t}]\end{aligned} \tag{31}$$

where t_0 is the initial time of rolling optimization; ΔT is the length of scheduling period of rolling optimization; k is the VPP number; C^i_{rev} represents the correction cost of VPPi; $P^i_{vppin,t,k}$ denotes the volume of power purchased from other VPPs by VPPi at time t; $P^i_{vppout,t,k}$ denotes the volume of power sold to other VPPs by VPPi at time t; $C^i_{mtrev,t}$ is the adjustment cost of MT in VPPi at time t, the formula of which meet Eq. (15); $C^i_{biorev,t}$ is the adjustment cost of BB in VPPi at time t, the formula of which meet Eq. (16); β_1 denotes the agency fee of VPPCO for unit of electricity; β_2 and β_3 denote the electricity prices for power purchase and sale between VPPs, respectively.

3.3.2. Constraints

(1) Electricity balance constraints

Eqs. (32)–(35) show the incremental balance of electricity.

$$\begin{aligned}\Delta P^i_{pv,t} + \Delta P^i_{wt,t} + \Delta P^i_{l,t} = \sum_{k=1,k\neq i}^{N}(P^i_{vppin,t,k} - P^i_{vppout,t,k}) \\ + P^i_{mtrev,t} - P^i_{mt,t} + P^i_{biorev,t} - P^i_{bio,t}\end{aligned} \tag{32}$$

$$\Delta P^i_{pv,t} = P^i_{pvrev,t} - \sum_{s=1}^{S} H^i_{t,s}P^i_{pv,t,s} \tag{33}$$

$$\Delta P^i_{wt,t} = P^i_{wtrev,t} - \sum_{s=1}^{S} H^i_{t,s}P^i_{wt,t,s} \tag{34}$$

$$\Delta P^i_{l,t} = P^i_{lrev,t} - \sum_{s=1}^{S} H^i_{t,s}P^i_{l,t,s} \tag{35}$$

where $P^i_{pvrev,t}$, $P^i_{wtrev,t}$, and $P^i_{lrev,t}$ are real-time forecasts of PV, WT output, and load in VPPi at time t, respectively; $\Delta P^i_{pv,t}$, $\Delta P^i_{wt,t}$, and $\Delta P^i_{l,t}$ are the forecast deviations of PV, WT output, and load in VPPi at time t; $P^i_{mtrev,t}$ and $P^i_{biorev,t}$ are the corrected outputs of MT and BB in VPPi at time t, and the constraints of which are consistent with constraints (20)–(24).

(2) Constraints of the energy interaction

Table 1
Interruptible load and shiftable load parameters.

Parameters	IL in VPP1	SL in VPP1	IL in VPP2	SL in VPP2	IL in VPP3	SL in VPP3
Maximum proportion	5%	7%	4%	8%	6%	6%
Maximum number of dispatches	10	8	8	10	8	8
Maximum number of consecutive dispatches	3	4	3	4	3	3

Constraints (36)–(37) ensures the power exchange in a time period do not exceed the maximum power transmission limit of lines, and constraints (38)–(39) restrict the power purchase or sale decision of VPP at time t. Constraint (40) ensures that a VPP cannot carry out the purchase and sale of electricity simultaneously, by not allowing bidirectional energy flow between two VPPs in the same time period.

$$0 \le P^{i}_{vppin,t,k} \le U^{i}_{in,t} P_{vpptra,\max} \tag{36}$$

$$0 \le P^{i}_{vppout,t,k} \le U^{i}_{out,t} P_{vpptra,\max} \tag{37}$$

$$0 \le P^{i}_{vppin,t,k} \le U^{i}_{in,t} \left| \Delta P^{k}_{pv,t} + \Delta P^{k}_{wt,t} + \Delta P^{k}_{l,t} \right| \tag{38}$$

$$0 \le P^{i}_{vppout,t,k} \le U^{i}_{out,t} \left| \Delta P^{k}_{pv,t} + \Delta P^{k}_{wt,t} + \Delta P^{k}_{l,t} \right| \tag{39}$$

$$U^{i}_{in,t} + U^{i}_{out,t} \le 1 \tag{40}$$

where $P_{vpptra,t,\max}$ denotes the maximum capacity of power transmission line; $U^{i}_{in,t}$ and $U^{i}_{out,t}$ are binary variables determine the energy interaction option of VPPi at time t, 1 means electricity is traded between VPPs, 0 means no energy interaction.

4. Case study

4.1. Basic data

In this case study, based on the MATLAB and GAMS platform, the proposed two-stage scheduling strategy with multi-time scale shown in Fig. 4 is validated under the environment of the Win10 operating system. The dispatch parameters of IL and SL are shown in Table 1, the unit technical parameters are shown in Table 2, and the operation parameters of VPPCO are shown in Table 3. A typical day in a residential area of Shanghai is selected to perform the day-ahead and real-time optimization scheduling. The residential area is assumed to have three VPPs (VPP1, VPP2, and VPP3) operating at different locations and three VPPs are put into operation. As the day-ahead forecasted load curves shown in Fig. 5, users in this area are classified as daily-night peak type users, night peak type users, and stationary type users. Those users are scheduled by VPP1, VPP2, and VPP3, the standard deviation of power load is set at 3% of the forecasted value. For the minimum and maximum hourly allowed power consumption of users, values of them are set at 95% and 105% of the hourly power load, respectively. Figs. 6–7 show the day-ahead and real-time forecasted wind power and photovoltaic output curves, the standard deviations of them are both set at 10% of their forecasted values. It is assumed that the contract price of power purchase signed in advance are 0.4¥/(kW h). The time-of-use price, and prices stipulated in the DR contract are shown in Fig. 8. For NG and biomass, the prices are assumed to be 3.5 ¥/m^3 and 1.2 ¥/kg.

4.2. Results analysis

Four cases designed to analyze various aspects of combined optimization of day-ahead and real-time stage are shown in Table 4. Case 1 considers the DR and VPPCO, and takes 4 h as the scheduling period of rolling optimization. With the same scheduling period, DR and VPPCO are not considered in case 2 and 3 respectively. Case 4 is the same as case 1 but with a different scheduling period of rolling optimization.

Table 2
Units parameters for VPP.

Parameters		Unit	Value
MTs	Ramping rate	kW/h	1000
	Descending rate	kW/h	1000
	Minimum output	kW	8000
	Maximum output	kW	500
	Start–stop cost	¥/kW	150
	Efficiency	–	0.285
	Emission factors of SO_2	kg/(kW h)	0.0036
	Emission factors of NOX	kg/(kW h)	0.025
	Emission factors of CO_2	kg/(kW h)	0.724
BBs	Minimum output	kW	10000
	Maximum output	kW	500
	Start–stop cost	¥/kW	120
	Efficiency	–	0.305
	Emission factors of SO_2	kg/(kW h)	0.0014
	Emission factors of NOX	kg/(kW h)	0.012
	Emission factors of CO_2	kg/(kW h)	0.429
ESS	Rated capacity	kW h	8000
	Initial capacity	kW h	4000
	Minimum SOC	–	0.1
	Maximum SOC	–	0.9
	Discharging efficiency	–	0.9
	Charging efficiency	–	0.9
	Rental cost	¥/(kW h)	0.52

Table 3
Operation parameters for VPPCO.

Parameters	Unit	Value
Operation cost of VPPCO	¥/kW	0.141
Power purchase price	¥/(kW h)	0.456
Power sale price	¥/(kW h)	0.462
Maximum line capacity	kW	1000

Table 4
Composition of four cases (✓ = components included, × = components excluded).

Case	DR	VPPCO	Scheduling period of rolling optimization (h)
1	✓	✓	4
2	×	✓	4
3	✓	×	4
4	✓	✓	8

4.2.1. Day-ahead scheduling results

To verify the accuracy and computing performance of the scenario elimination proposed in this paper, VPP1 in case 1 is taken as an example, and the 10, 50, 100, and 150 scenarios is selected after the elimination, respectively. Table 5 shows the total profit and computation time in the day-ahead stage. As shown in Table 5, the number of scenarios has little effect on the total profit, with 150 scenarios compared to 10 scenarios, the total profit only increases by 0.49%. However, the computation time increases significantly from 0.843 s to 1004 s. It can be seen that the simulation with 10 scenarios has a good solution accuracy and computation time. Considering the computational burden in the VPP scheduling stage, 10 scenarios are selected for the following analysis.

Fig. 9 shows the dispatch results of SL and IL in case 1. Load in VPP1 is transferred from hour of 12–13 and 20–21 to hour of 5–6 and 15–16, and the interrupted loads are accumulated around hour of 11–13 and hour of 18–20. The volume of the load

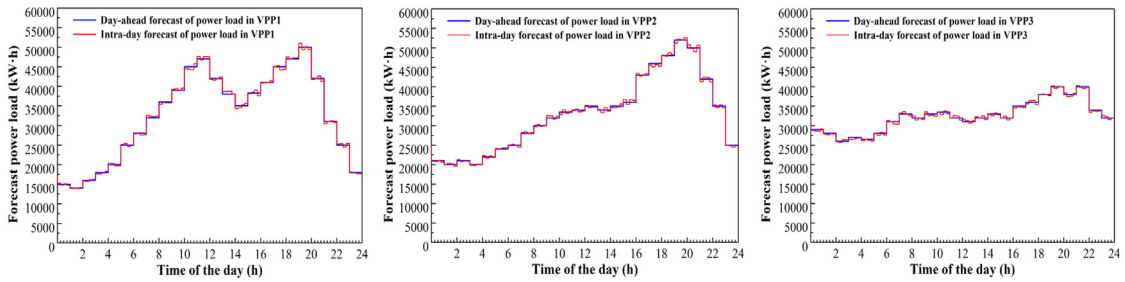

(a) Forecast power load in VPP1 (b) Forecast power load in VPP2 (c) Forecast power load in VPP3

Fig. 5. Forecast power load in VPPs.

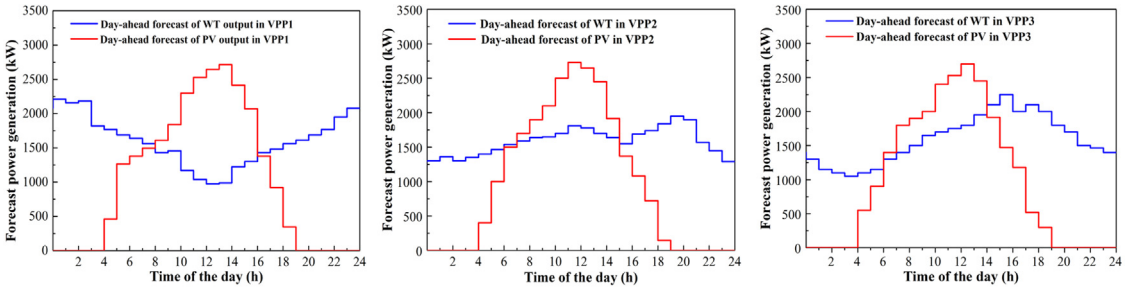

(a) Forecast power generation in VPP1 (b) Forecast power generation in VPP2 (c) Forecast power generation in VPP3

Fig. 6. Forecast power generation in the day-ahead stage.

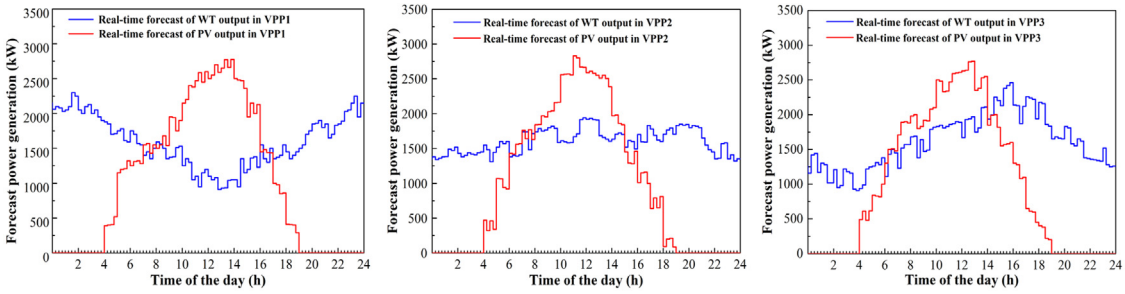

(a) Forecast power generation in VPP1 (b) Forecast power generation in VPP2 (c) Forecast power generation in VPP3

Fig. 7. Forecast power generation in the real-time stage.

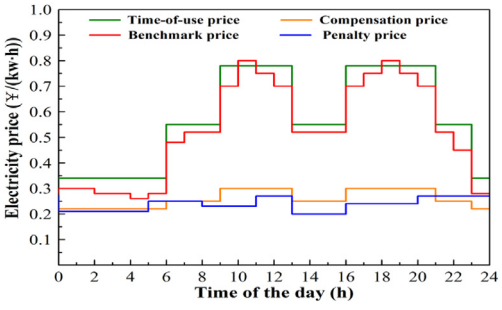

Fig. 8. Electricity prices for VPPs.

Table 5
Comparison of different scenarios of VPP1 in case 1.

Number of selected scenarios	10	50	100	150
Total profit (¥)	183,033	183,356	183,604	183,929
Computation time (s)	0.843	65	338	1004

transferred and interrupted in VPP1 is balanced. The reason is that two electricity consumption peaks in VPP1 are in the periods of high benchmark electricity price, and the compensation price is at high at the time as well, which encourages the consumers to accept the DR offer and make a move. Load in VPP2 is transferred from hour of 20–22 to hour of 4–6 and 9–10, and interrupted during hour of 21–23. It should be noted that the volume of load shifted obviously exceeds the load interrupted, that is because the peak of electricity usage in VPP1 coincides with the peak of benchmark electricity price, while the compensation price is not at its peak, which makes consumers more inclined to shift loads to other periods with lower benchmark electricity price. For VPP3, the load is transferred from hour 14 and 16 to hour 1 and 4, and interrupted at hour 8, 20, and 22. It can be seen that the dispatch of load is dispersed and not concentrated in a certain period of time. Moreover, the number of load dispatched in VPP3 is less than the numbers in the previous two VPPs. They can be attributed to the lower load fluctuations, which results in the effect of DR not being significant. In general, the load dispatch of VPP1-3 indicates that under the guidance of the benchmark price and the incentive of the compensation price, users tend to reasonably reduce their electricity usage at peak hours, while

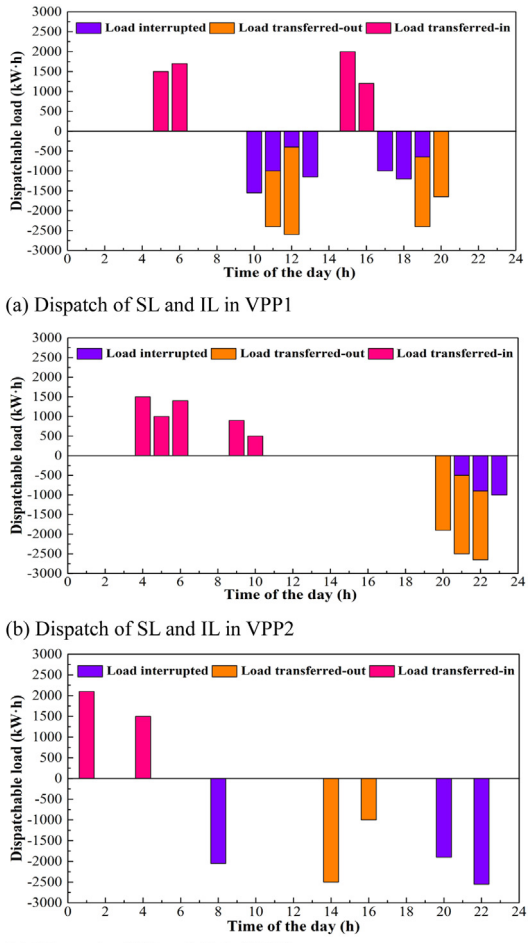

(a) Dispatch of SL and IL in VPP1

(b) Dispatch of SL and IL in VPP2

(c) Dispatch of SL and IL in VPP3

Fig. 9. Load dispatch for VPPs.

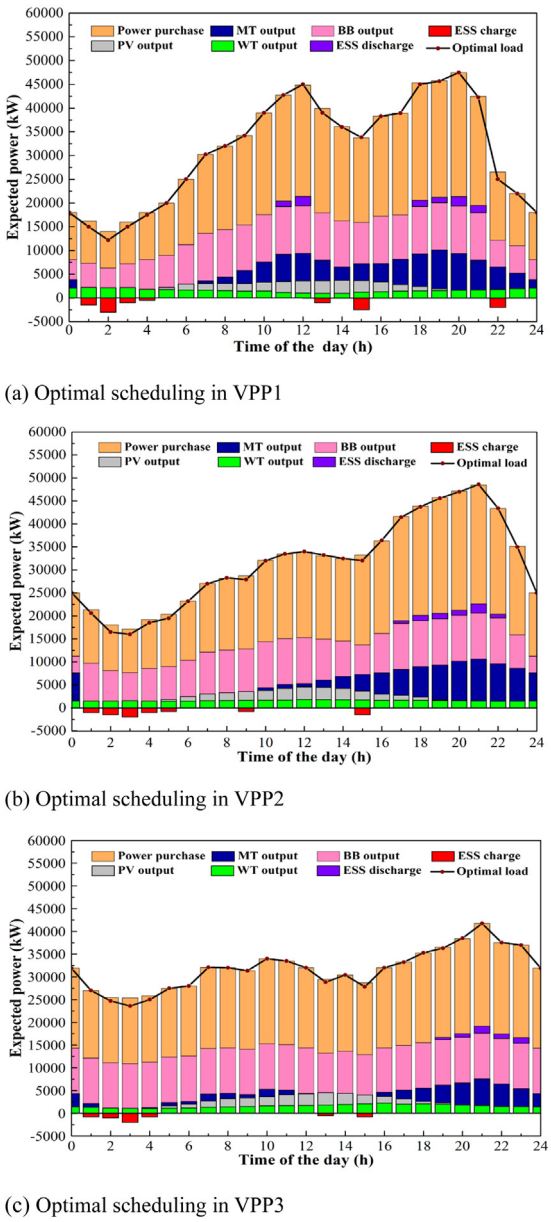

(a) Optimal scheduling in VPP1

(b) Optimal scheduling in VPP2

(c) Optimal scheduling in VPP3

Fig. 10. Optimal day-ahead scheduling for VPPs.

flexibly transferring loads to periods with low electricity prices, which is conducive to the optimized power load distribution and the reduced peak-to-valley difference.

Fig. 10 shows the optimal day-ahead scheduling for VPPs in case 1. It can be seen that the BB has the priority in operation, that is because it has lower operating and environmental cost compared to MT. It is worth noting that both MT and BB increase their output during peak load periods, while for economical efficiency, MT ceases its operation during some periods of the valley load. Especially during hour of 1–4, there is no power generation from PV and loads of the three VPPs are at a lower valley, VPPs tend to purchase power from the electricity market to reduce the output of BB and avoid frequent start–stops for MT. For ESS, it is charged at the daytime when the penetration rate of renewable energy is high or at night when both the load and electricity price are low. Conversely, it is discharged when the load and electricity price are high, so as to meet the load demand at peak period.

4.2.2. Economic analysis of DR

Table 6 is a comparative analysis of case 1 and 2, which shows the day-ahead revenues and costs of VPPs after and before the DR. For the costs of power purchase and revenues from power sale, decreases are seen in the three VPPs after DR. The decline in costs can be attributed by the demand reduction of power purchase, which is resulted from the load interruption. Moreover, the operation costs of VPPs in case 1 is lower than those in case 2. It can be attributed by the peak load shifting through load transfer and interruption, which reduces the output of controllable units during peak periods and avoids the frequent start and stop operations during valley periods. The total profits increase after participating in DR, rising by 6.65%, 5.87%, and 4.54% in VPP1-3, respectively, and the computation time also increases. Considering that the computation time is at the millisecond level, it can fully meet the requirements of day-ahead scheduling. Combining Fig. 9 and Table 6, it can be seen that the DR brings significant economic benefits while optimizing the power load distribution.

4.2.3. Economic analysis of VPPCO

By comparing the scheduling results of cases 1 and 3, the effects of VPPCO for the real-time correction can be obtained. As shown in Table 7, the total correction cost in case 3 is higher than that in case 1, mainly because the adjustment expenses of MT and BB in case 3 cost much more. Since only the outputs of controllable units are adjusted in case 3, without considering the coordination role of VPPCO, MT and BB are forced to start and

Table 6
Economic analysis of DR in the day-ahead stage.

Cases	VPP number	Power purchase cost (¥)	Power sale revenue (¥)	Compensation cost (¥)	Penalty income (¥)	VPP operation cost (¥)	Total profit (¥)	Computation time (ms)
1	VPP1	78,519	428,824	2,006	969	166,235	183,033	843
	VPP2	80,047	435,213	1,358	814	165,148	189,474	815
	VPP3	80,216	412,325	1,823	825	145,117	185,994	771
2	VPP1	82,504	434,289	–	–	180,168	171,617	613
	VPP2	83,125	442,106	–	–	180,014	178,967	697
	VPP3	81,121	416,421	–	–	157,386	177,914	618

Table 7
Economic analysis of VPPCO.

Cases	VPP number	Revenue from power sale (¥)	Cost of power purchase (¥)	Operation cost of VPPCO (¥)	Adjustment cost of MT (¥)	Adjustment cost of BB (¥)	Total cost (¥)	Computation time (s)
1	VPP1	6,581	8,955	4,777	70,509	70,588	148,248	21
	VPP2	9,394	6,858	4,987	66,450	72,609	141,510	23
	VPP3	8,755	7,397	4,959	46,709	84,077	134,387	20
3	VPP1	–	–	–	79,874	80,578	160,452	14
	VPP2	–	–	–	71,645	77,847	149,492	16
	VPP3	–	–	–	52,127	90,753	142,880	14

Table 8
Economic analysis of increased scheduling period.

VPP number	Revenue from power sale (¥)	Cost of power purchase (¥)	Operation cost of VPPCO (¥)	Adjustment cost of MT (¥)	Adjustment cost of BB (¥)	Total cost (¥)	Computation time (s)
VPP1	7,015	9,427	5,932	65,477	66,149	139,970	26
VPP2	9,686	7,145	6,046	63,645	67,543	134,693	29
VPP3	8,913	7,549	6,018	42,869	80,247	127,770	25

stop frequently to balance the forecast deviations, which results in the significantly increased start–stop cost. Moreover, the total cost of VPP1 is reduced by the most, at 8.23%, exceeding 5.64% of VPP2 and 6.32% of VPP3. As shown in Fig. 7, the wind power of VPP1 is lower during the peak of the daytime electricity usage, which allows MT and BB to take on more output, so as to meet the power demand. Hence, controllable units in VPP1 are more susceptible to the forecast deviation. Although the computation time increases as the internal power trading coordinated by the VPPCO is taken into account, the complementary energy mitigates the impact of real-time scheduling on the output adjustment of MT and BB in the real-time stage, which accounts for the greatest decrease of correction cost in VPP1.

4.2.4. Economic analysis of rolling optimization

Compared to case 1, the scheduling period of rolling optimization is doubled in case 4. The extended scheduling period means that the VPP can obtain more forecast information of the future time periods before making decisions, which is conducive to improving the scheduling scheme in the real-time stage. Fig. 11 illustrates details of the power exchange in case 1 and 4. As shown in Fig. 11, in comparison with case 1, case 4 exists a rise in the flexibility and volume of power purchased and sold. In view of the increase in the response time and power information about energy complementation after the extension of the scheduling period, it can be attributed to the adequate response of energy interaction to the real-time dispatch instructions. It is can be seen from Table 8 that the total correction cost decreases with the increase of the scheduling period, dropped by 5.58%, 4.82%, and 4.92% in VPP1, 2, and 3, respectively, and the costs of MT and BB decrease the most, that is because the optimization of power trading under the improved scheduling plan in case 4, thereby enhancing the effect of energy complementarity and reducing the adjustment of controllable unit output. However, due to the increase in the number of variables that need to be computed with the extension of the scheduling period, the computation time increases and the computation efficiency decreases correspondingly. Therefore, in the real-time stage, the VPP needs to weigh the economic and computational efficiency according to its actual condition, so as to select an appropriate rolling optimization scheduling period.

5. Conclusion

This paper proposes a two-stage scheduling strategy for VPP with multi-time scale optimization, and the two scheduling strategies are closely linked and collaboratively optimized. Multiple cases are set up for comparative analysis, and the conclusions are as follows:

(a) Under the premise of meeting power demand and ensuring users' satisfaction, DR improves the ability of power consumers to actively respond and flexibly participate in the VPP dispatch and brings considerable economic benefits. Moreover, the distribution of power load is optimized and the peak-to-valley difference is properly stabilized, which is conducive to the operational safety of VPP.

(b) The VPPCO plays a vital role in the real-time stage. It is manifested in the fact that the energy complementation between VPPs is achieved by the VPPCO coordination, which significantly improves economic efficiency and promotes the adequate consumption of regional energy. Through the rolling optimization for the real-time correction, scheduling schemes can be formulated more accurately and reasonably, and the economy and flexibility of the system operation can be greatly improved.

(c) By tracking the pollutant gas emissions of the aggregated units, the environmental cost is considered in this paper. In general, the environmental cost is aimed at pursuing a balance between economy and environmental protection, which restricts the output of controllable units, thereby promoting the full utilization of renewable energy. Furthermore, the real-time correction balances the forecast deviation of wind power, photovoltaics and load, and the waste of wind power and photovoltaics

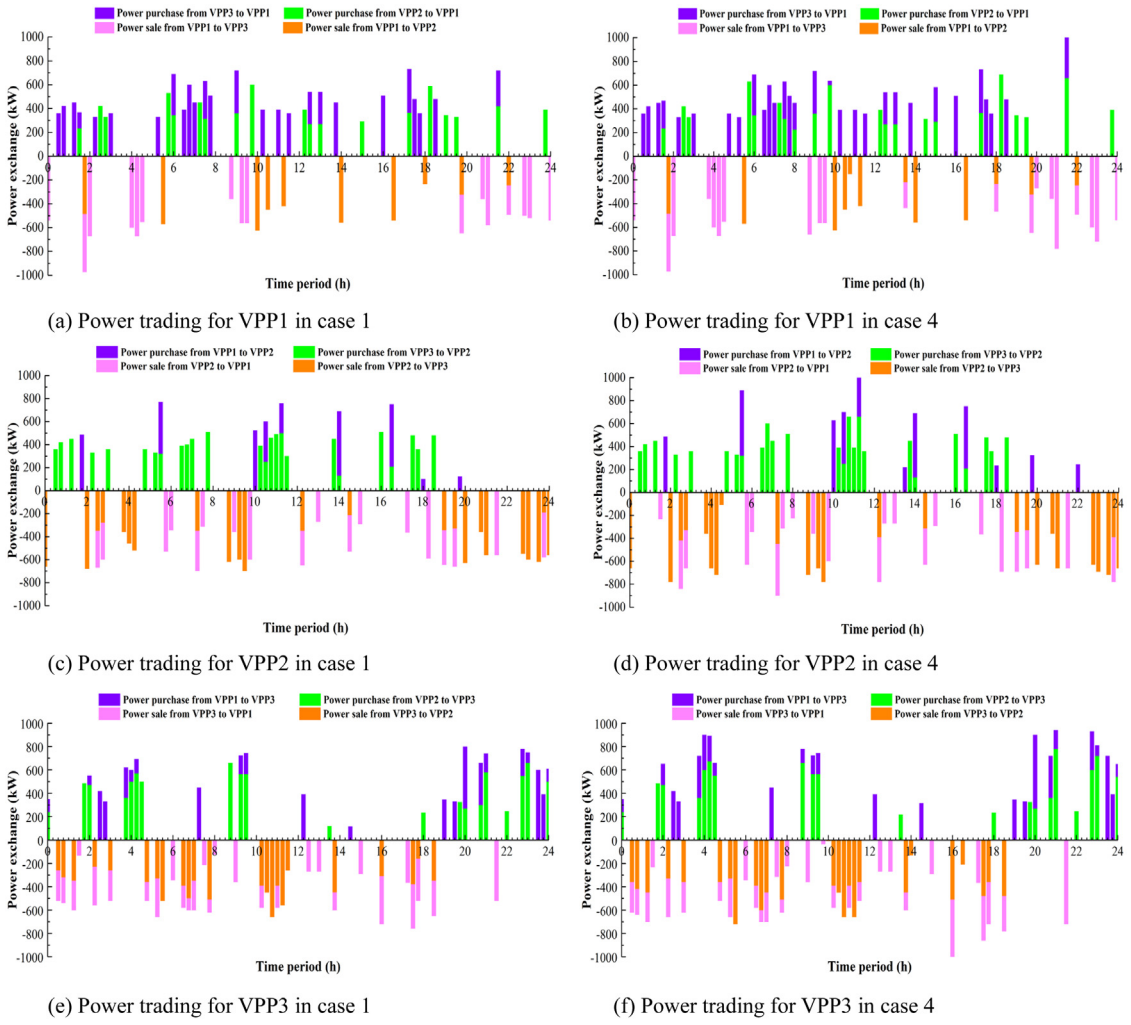

(a) Power trading for VPP1 in case 1

(b) Power trading for VPP1 in case 4

(c) Power trading for VPP2 in case 1

(d) Power trading for VPP2 in case 4

(e) Power trading for VPP3 in case 1

(f) Power trading for VPP3 in case 4

Fig. 11. Energy interactions coordinated by VPPCO in case 1 and 4.

can be effectively mitigated, so as to maximize the low-carbon performance of VPP. Therefore, the optimal scheduling strategy proposed in this paper can be served as the reference for the practical application of the environment-friendly VPP.

With the continuous progress of VPP, higher requirements have been put forward for the research on the economical, eco-friendly, and safe operation. In this paper, the two-stage optimization of the VPP is only preliminarily studied. There is still a lot of research space, and many aspects are simplified due to the limited ability and time, such as the line loss, and the application of artificial intelligence technology in the process of model solving. In the future work, we will consider the impact of line loss, and explore the collaborative optimization of VPP power generation and distribution based on the distribution network system. Moreover, the further improvements in computing performance with artificial intelligence algorithms will be taken into account in the subsequent work. On this basis, the dynamic optimization of the scheduling period in the real-time stage will be studied to balance economic and computational efficiency.

CRediT authorship contribution statement

Jinye Cao: Methodology, Writing – original draft. **Yingying Zheng:** Visualization, Writing – review & editing. **Xueru Han:** Investigation, Data curation. **Dechang Yang:** Conceptualization, Project administration, Writing – review & editing. **Jianshu Yu:** Writing – review & editing. **Nikita Tomin:** Writing – review & editing. **Payman Dehghanian:** Writing – review & editing.

Declaration of competing interest

The authors declare that they have no known competing financial interests or personal relationships that could have appeared to influence the work reported in this paper.

Acknowledgments

This work was supported by the National Natural Science Foundation of China under grand numbers (No. 51977212) and (No. U2166208).

References

Aalami, H.A., Moghaddam, M.P., Yousefi, G.R., 2010. Modeling and prioritizing demand response programs in power markets. Electric. Power Syst. Res. 80 (4), 426–435.

Akkaş, Ö.P., Çam, E., 2020. Optimal operational scheduling of a virtual power plant participating in day-ahead market with consideration of emission and battery degradation cost. Int. Trans. Electric. Energy 30 (7).

Asl, S.A.F., Bagherzadeh, L., Pirouzi, S., Norouzi, M., Lehtonen, M., 2021. A new two-layer model for energy management in the smart distribution network containing flexi-renewable virtual power plant. Electr. Power Syst. Res. 194, 107085.

Castillo, A., Flicker, J., Hansen, C.W., Watson, J.P., Johnson, J., 2019. Stochastic optimisation with risk aversion for virtual power plant operations: A rolling horizon control. IET Gener., Transm. Distrib. 13 (11), 2063–2076.

Chen, W., Qiu, J., Chai, Q., 2021. Customized critical peak rebate pricing mechanism for virtual power plants. IEEE Trans. Sustain. Energy 12 (4), 2169–2183.

Dou, X., Shao, Y., Wang, J., Hu, Q., 2021. Heat-electricity joint bidding strategies for intelligent buildings in intelligent building cluster. Int. J. Electr. Power 129, 106891.

Du, N., Liu, Y., Liu, Y., 2021. A new data-driven distributionally robust portfolio optimization method based on wasserstein ambiguity set. IEEE Access 9, 3174–3194.

Du, W., Zhong, W., Tang, Y., Du, W., Jin, Y., 2019. High-dimensional robust multi-objective optimization for order scheduling: A decision variable classification approach. IEEE Trans. Ind. Inf. 15 (1), 293–304.

Gomes, I.L.R., Melicio, R., Mendes, V.M.F., 2021. A novel microgrid support management system based on stochastic mixed-integer linear programming. Energy 223, 120030.

Grimm, F., Kolahian, P., Zhang, Z., Baghdadi, M., 2021. A sphere decoding algorithm for multistep sequential model-predictive control. IEEE Trans. Ind. Appl. 57 (3), 2931–2940.

Hadayeghparast, S., SoltaniNejad Farsangi, A., Shayanfar, H., 2019. Day-ahead stochastic multi-objective economic/emission operational scheduling of a large scale virtual power plant. Energy 172, 630–646.

Huang, Z., 2014. Evaluating intelligent residential communities using multi-strategic weighting method in China. Energ Build. 69, 144–153.

Jha, B.K., Singh, A., Kumar, A., Misra, R.K., Singh, D., 2021. Phase unbalance and PAR constrained optimal active and reactive power scheduling of virtual power plants (VPPs). Int. J. Electr. Power 125, 106443.

Ju, L., Tan, Q., Lu, Y., Tan, Z., Zhang, Y., Tan, Q., 2019. A CVaR-robust-based multi-objective optimization model and three-stage solution algorithm for a virtual power plant considering uncertainties and carbon emission allowances. Int. J. Electr. Power 107, 628–643.

Ju, L., Tan, Z., Yuan, J., Tan, Q., Li, H., Dong, F., 2016. A bi-level stochastic scheduling optimization model for a virtual power plant connected to a wind–photovoltaic–energy storage system considering the uncertainty and demand response. Appl. Energy 171, 184–199.

Lyu, Xu, Wang, Fu, 2019. A two-layer interactive mechanism for peer-to-peer energy trading among virtual power plants. Energies (Basel) 12 (19), 3628.

Mishra, A.K., Jokisalo, J., Kosonen, R., Kinnunen, T., Ekkerhaugen, M., Ihasalo, H., Martin, K., 2019. Demand response events in district heating: Results from field tests in a university building. Sustain. Cities Soc. 47, 101481.

Mohy Ud Din, G., Muttaqi, K.M., Sutanto, D., 2019. Transactive energy-based planning framework for VPPs in a co-optimised day-ahead and real-time energy market with ancillary services. IET Gener., Transm. Distrib. 13 (11), 2024–2035.

Naughton, J., Wang, H., Riaz, S., Cantoni, M., Mancarella, P., 2020. Optimization of multi-energy virtual power plants for providing multiple market and local network services. Electr. Power Syst. Res. 189, 106775.

Nguyen, H.T., Le, L.B., Wang, Z., 2018. A bidding strategy for virtual power plants with the intraday demand response exchange market using the stochastic programming. IEEE Trans. Ind. Appl. 54 (4), 3044–3055.

Niknam, T., Azizipanah-Abarghooee, R., Narimani, M.R., 2012. An efficient scenario-based stochastic programming framework for multi-objective optimal micro-grid operation. Appl. Energy 99, 455–470.

Rahimi, M., Ardakani, F.J., Olatujoye, O., Ardakani, A.J., 2022. Two-stage interval scheduling of virtual power plant in day-ahead and real-time markets considering compressed air energy storage wind turbine. J. Energy Storage 45, 103599.

Royapoor, M., Pazhoohesh, M., Davison, P.J., Patsios, C., Walker, S., 2020. Building as a virtual power plant, magnitude and persistence of deferrable loads and human comfort implications. Energ Build. 213, 109794.

Seljom, P., Kvalbein, L., Hellemo, L., Kaut, M., Ortiz, M.M., 2021. Stochastic modelling of variable renewables in long-term energy models: Dataset. Scenario Gener. Qual. Results, Energy 236, 121415.

Shayegan-Rad, A., Badri, A., Zangeneh, A., 2017. Day-ahead scheduling of virtual power plant in joint energy and regulation reserve markets under uncertainties. Energy 121, 114–125.

Sheng, B., Xu, B., Pan, Y., Chen, H., 2021. How to efficiently promote distributed energy resources in China: Using a nonparametric econometric method. J. Clean. Prod. 285, 125420.

Vagropoulos, S.I., Kardakos, E.G., Simoglou, C.K., Bakirtzis, A.G., Catalão, J.P.S., 2016. ANN-based scenario generation methodology for stochastic variables of electric power systems. Electr. Power Syst. Res. 134, 9–18.

Vahedipour-Dahraie, M., Rashidizadeh-Kermani, H., Anvari-Moghaddam, A., Siano, P., 2020. Risk-averse probabilistic framework for scheduling of virtual power plants considering demand response and uncertainties. Int. J. Electr. Power 121, 106126.

Vahedipour-Dahraie, M., Rashidizadeh-Kermani, H., Shafie-Khah, M., Catalao, J.P.S., 2021. Risk-averse optimal energy and reserve scheduling for virtual power plants incorporating demand response programs. IEEE Trans. Smart Grid 12 (2), 1405–1415.

Wang, S., Wu, W., 2021. Aggregate flexibility of virtual power plants with temporal coupling constraints. IEEE Trans. Smart Grid 12 (6), 5043–5051.

Wang, X., Zhang, H., Zhang, S., Wu, L., 2021. Impacts of joint operation of wind power with electric vehicles and demand response in electricity market. Electr. Power Syst. Res. 201, 107513.

Xiao, C., Sutanto, D., Muttaqi, K.M., Zhang, M., 2020. Multi-period data driven control strategy for real-time management of energy storages in virtual power plants integrated with power grid. Int. J. Electr. Power 118, 105747.

Yan, M., He, Y., Shahidehpour, M., Ai, X., Li, Z., Wen, J., 2019. Coordinated regional-district operation of integrated energy systems for resilience enhancement in natural disasters. IEEE Trans. Smart Grid 10 (5), 4881–4892.

Yang, D., He, S., Chen, Q., Li, D., Pandzic, H., 2019. Bidding strategy of virtual power plant considering carbon-electricity trading. CSEE J. Power Energy Syst..

Yang, D., Wang, M., Yang, R., Zheng, Y., Pandzic, H., 2021. Optimal dispatching of an energy system with integrated compressed air energy storage and demand response. Energy 234, 121232.

Yi, Z., Xu, Y., Gu, W., Wu, W., 2020. A multi-time-scale economic scheduling strategy for virtual power plant based on deferrable loads aggregation and disaggregation. IEEE Trans. Sustain. Energy 11 (3), 1332–1346.

Yu, J., Yang, D., Chen, Z., 2021. Multi-energy flow calculation based on energy cell and parallel distributed computation. Int. J. Electr. Power 131, 107147.

Yuan, Y., Wei, Z., Sun, G., Sun, Y., Wang, D., 2014. A real-time optimal generation cost control method for virtual power plant. Neurocomputing 143, 322–330.

Zamani, A.G., Zakariazadeh, A., Jadid, S., 2016a. Day-ahead resource scheduling of a renewable energy based virtual power plant. Appl. Energy 169, 324–340.

Zamani, A.G., Zakariazadeh, A., Jadid, S., Kazemi, A., 2016b. Stochastic operational scheduling of distributed energy resources in a large scale virtual power plant. Int. J. Electric Power 82, 608–620.

Zhang, G., Jiang, C., Wang, X., 2019. Comprehensive review on structure and operation of virtual power plant in electrical system. IET Gener., Transm. Distrib. 13 (2), 145–156.

Zheng, Y., Jenkins, B.M., Kornbluth, K., Træholt, C., 2018. Optimization under uncertainty of a biomass-integrated renewable energy microgrid with energy storage. Renew. Energy 123, 204–217.

Zhou, B., Liu, X., Cao, Y., Li, C., Chung, C.Y., Chan, K.W., 2016. Optimal scheduling of virtual power plant with battery degradation cost. IET Gener., Transm. Distrib. 10 (3), 712–725.

Zhou, Y., Wei, Z., Shahidehpour, M., Chen, S., 2021. Distributionally robust resilient operation of integrated energy systems using moment and wasserstein metric for contingencies. IEEE Trans. Power Syst. 36 (4), 3574–3584.

Zhu, J., Duan, P., Liu, M., Xia, Y., Guo, Y., Mo, X., 2019. Bi-level real-time economic dispatch of VPP considering uncertainty. IEEE Access 7, 15282–15291.